JACS
JOURNAL OF THE AMERICAN CHEMICAL SOCIETY
Communication
pubs.acs.org/JACS

Surface-Modified Silicon Nanoparticles with Ultrabright Photoluminescence and Single-Exponential Decay for Nanoscale Fluorescence Lifetime Imaging of Temperature

Qi Li,[†] Yao He,[‡] Jian Chang,[§] Lei Wang,[⊥] Hongzheng Chen,[∥] Yan-Wen Tan,[§] Haiyu Wang,[⊥] and Zhengzhong Shao*,[†]

[†]State Key Laboratory of Molecular Engineering of Polymers, Advanced Material Laboratory, Department of Macromolecular Science, Fudan University, Shanghai 200433, P. R. China

[‡]Institute of Functional Nano & Soft Materials (FUNSOM) and Jiangsu Key Laboratory for Carbon-based Functional Materials & Devices, Soochow University, Suzhou 215123, P. R. China

[§]State Key Laboratory of Surface Physics and Department of Physics, Fudan University, Shanghai 200433, China

[⊥]State Key Laboratory on Integrated Optoelectronics and College of Electronic Science and Engineering, Jilin University, Changchun 130012, China

[∥]State Key Laboratory of Silicon Materials and Department of Polymer Science and Engineering, Zhejiang University, Hangzhou 310027, P. R. China

Supporting Information

ABSTRACT: In this Communication, we report fabrication of ultrabright water-dispersible silicon nanoparticles (SiNPs) with quantum yields (QYs) up to 75% through a novelly designed chemical surface modification. A simple one-pot surface modification was developed that improves the photoluminescent QYs of SiNPs from 8% to 75% and meanwhile makes SiNPs water-dispersible. Time-correlated single photon counting and femtosecond time-resolved photoluminescence techniques demonstrate the emergence of a single and uncommonly highly emissive recombination channel across the entire NP ensemble induced by surface modification. The extended relatively long fluorescence lifetime (FLT), with a monoexponential decay, makes such surface-modified SiNPs suitable for applications involving lifetime measurements. Experimental results demonstrate that the surface-modified SiNPs can be utilized as an extraordinary nanothermometer through FLT imaging.

Silicon nanoparticles (SiNPs) have attracted increasing interest in many fields due to their intrinsic advantages, e.g., high abundance, low cost, minimal toxicity, favorable biocompatibility, and compatibility with silicon technologies.[1] When desirable properties are obtained, SiNPs are widely accepted as potentially promising alternatives to the typically used heavy-metal-containing II−VI quantum dots (QDs) in fields such as optoelectronics and biomedicine.[2] However, when it comes to optical properties, SiNPs still fall behind the direct band-gap-based QDs (e.g., lower photoluminescence (PL) efficiency).[3] Thus, for SiNPs, it remains crucial to seek effective ways to improve their optical properties and further tap their potential for valuable applications.

Temperature sensing is a necessity in widespread applications: integrated photonic devices, nano/micro electronics, biology, medical diagnostics, etc. As modern science and technology comes into the nano/micro scale, temperature sensing on a localized small length scale becomes a pressing need for the scientific community.[4] In this context, use of nanoscale fluorescence temperature probes is regarded as the most promising method for temperature sensing.[5] In recent years, interest in sensing or imaging by the fluorescence lifetime (FLT) technique has been increasing because FLT is less dependent on several factors (e.g., fluorophore concentration, photobleaching, fluorescent background, and spectral overlap) that perturb intensity measurements, making it a preferred parameter in fluorescence sensing and imaging for many practical applications.[6a] Unfortunately, QDs are rarely used in this domain because most exhibit complicated multiple-exponential decays due to, e.g., excitonic states, surface, etc. This makes it very difficult to get accurate information from FLT measurements.[6b]

Herein, through a simple yet novel surface modification, ultrabright cyan-green fluorescence with PL quantum yields (QYs) up to 75% can be readily obtained from water-dispersible SiNPs. A novel, highly emissive recombination channel across the entire NP ensemble was induced by such surface modification. The surface-modified SiNPs possess an extended, relatively long FLT with a monoexponential decay, which was utilized for accurate and sensitive nanoscale fluorescence imaging of temperature. SiNPs with surface Si−Cl bonds (Cl-SiNPs) were first prepared by the solution-reduction method modified by Kauzlarich's group.[7] Diphenylamine (di) and carbazole (ca) were chosen to modify the SiNPs while the surface was undergoing oxidation simultaneously (Figure 1a). The design of the diphenylamine-modified SiNPs (di-SiNPs) and carbazole-modified SiNPs (ca-SiNPs) is based on the following considerations: (1) diphenylamine and carbazole, nitrogen-containing aromatic electron-rich systems with high nucleophil-

Received: July 22, 2013
Published: September 13, 2013

dx.doi.org/10.1021/ja407508v | J. Am. Chem. Soc. 2013, 135, 14924−14927

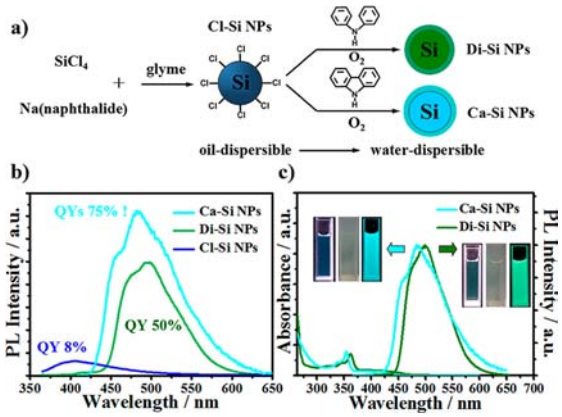

Figure 1. Surface-modified water-dispersible SiNPs with ultrabright fluorescence. (a) Scheme of solution reduction syntheses and novelly designed surface modification to make highly luminescent water-dispersible SiNPs. (b) PL spectra of SiNPs before and after surface modification (λ_{ex} = 360 nm, 20 °C). (c) Normalized PL and UV−visible absorption spectra of the two surface-modified SiNPs. Insets: Photographs of dilute sample solutions dispersed with the ca-SiNPs (left) and di-SiNPs (right). From left to right are photographs of sample solution under sunlight in black background, in normal conditions, and under 365 nm UV photoexcitation, respectively.

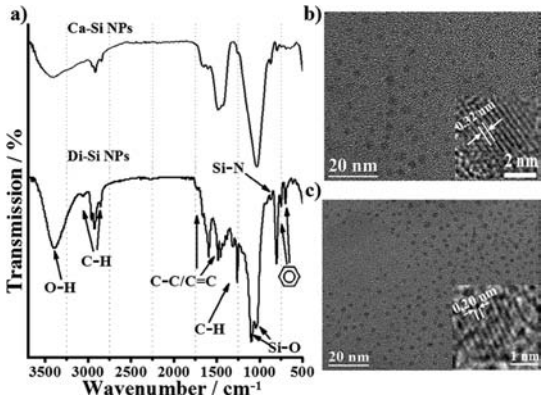

Figure 2. Characterization of the two surface-modified SiNPs. (a) FTIR spectra of SiNPs with the assignment of characteristic peaks. (b) TEM overview images of ca-SiNPs. A single NP is enlarged in the inset with a spacing of about 3.20 Å, consistent with diamond lattice Si (111). (c) TEM overview images of di-SiNPs. A single NP is enlarged in the inset with a spacing of about 2.00 Å, consistent with diamond lattice Si (220).

icity, can easily react with the surface Si−Cl bonds and hold great potential to improve and modulate the PL properties.[8] (2) *In situ* surface oxidation can make SiNPs water-dispersible, and the partially oxidized surface can be more reactive with diphenylamine due to the polarization effect of surface bonds.[9]

It is worth noting that such surface modifications lead to distinct changes in the optical properties of SiNPs. Typically, in comparison to those of unmodified SiNPs, the maximum emission peak of di-SiNPs is distinctly shifted from 405 to 500 nm, and the PLQYs is strongly enhanced by more than 5 times up to 50% at room temperature (Figure 1b). More significantly, for ca-SiNPs, ultrabright cyan fluorescence at 480 nm with PLQYs up to 75% can be obtained (Figure 1b). Such ultrabright fluorescence can be clearly observed even under sunlight (Figure 1c, inset). Figure 1c displays a clearly resolved absorption peak of the electronic transition and a symmetrical PL peak, indicating superb optical properties of the two surface-modified SiNPs. Both of the surface-modified SiNPs can be readily dispersed in acidic and neutral water; however, they aggregate as the pH increases to strong base, along with significant PL quenching (more details are described in Figures S1 and S2). In addition, such resultant SiNPs feature robust storage stability, exhibiting only about 20% loss of PL intensity after prolonged storage for 5 months in the ambient environment free of any special protection (Figure S3). Until now, SiNPs are still regarded poorly as lower yield emitters compared with cadmium-based QDs, especially for water-dispersible SiNPs.[2,3] Although PLQYs up to 60% have been reported in previous studies, such SiNPs can be dispersed only in nonpolar solvents and hold strong PL only in the deep red region with limited stability.[10] Therefore, our work provides an effective and simple method in terms of designed surface modification to realize ultrabright PL from SiNPs. Such ultrabright PL and high storage stability in atmospheric environment, together with good dispersibility in aqueous solutions, may lead to widespread applications such as light-emitting devices and biological imaging.

Surface modification was examined by Fourier transform infrared (FTIR) spectroscopy, ^{1}H NMR spectroscopy, and X-ray photoelectron spectroscopy (XPS). In particular, FTIR spectra (Figure 2a) demonstrate the attachment of diphenylamine or carbazole (aromatic C−H bands 3015−2850 and 1400−2000 cm^{-1}, Si−N bonds 840 cm^{-1}) and oxidation (Si−O−Si vibrations at 1000−1200 cm^{-1}, Si−OH vibrations at 3200−3600 cm^{-1}) on the surface of SiNPs.[11] ^{1}H NMR results (Figure S4) also demonstrate the attachment of capping agents. XPS analysis of SiNPs shows the expected Si, O, and C elemental signatures as well as a low-intensity emission in the N 1s spectral region (Figure S5).[8] Transmission electron microscopy (TEM) images demonstrate the presence of the two surface-modified SiNPs (Figure 2b,c, inset is an enlarged image of a single NP). A region including this TEM observation area was analyzed by energy-dispersive X-ray spectroscopy (Figure S6) and selected-area electron diffraction pattern (Figure S7). The size distributions, calculated by measuring more than 300 particles, show that the di-SiNPs have an average size of 2.40 ± 0.65 nm (Figure S8), and the ca-SiNPs have an average size of 2.49 ± 0.67 nm (Figure S9).

To understand the mechanism underlying the dramatic improvement in emission efficiency in such surface-modified SiNPs, we studied PL dynamics of the SiNPs before and after surface modification through the time-correlated single photon counting (TCSPC) technique. As shown in Figure 3a, the PL decay is biexponential in unmodified SiNPs with an average FLT of 4 ns. Interestingly, both surface modifications completely eliminate the fast PL component and result in a single-exponential decay with increased FLT (di-SiNPs, 17 ns; ca-SiNPs, 31 ns). Meanwhile, a spectrally uniform single-exponential decay was observed across the whole emission profile (Figure 3b). Generally, rapid nonradiative processes such as surface traps result in decreasing PLQYs and FLT. The strongly enhanced PLQYs and significantly increased FLT, together with the monoexponential decay, suggest effective suppression of originally existing rapid nonradiative decay processes and emergence of a single highly emissive recombination channel across the entire QD ensemble through the surface modification (Figure 3d). To further scrutinize the origin of the ultrabright fluorescence, sub-picosecond time-resolved fluorescence dynamics were measured by fluorescence upconversion at 400 nm excitation to observe the faster process (Figure 3c). Both of the surface-modified SiNPs have a long PL lifetime,

dx.doi.org/10.1021/ja407508v | J. Am. Chem. Soc. 2013, 135, 14924−14927

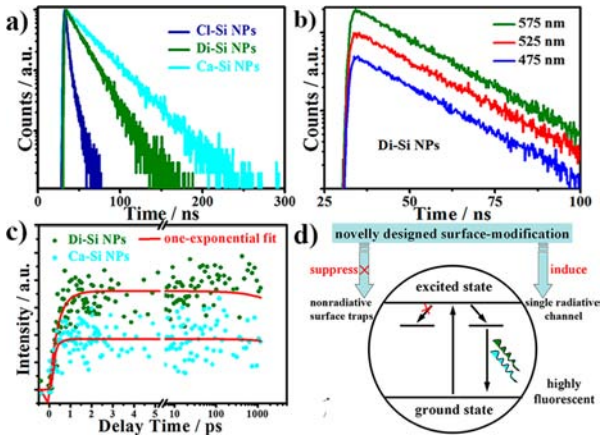

Figure 3. TCSPC and femtosecond time-resolved PL techniques to unravel the mechanism leading to ultrabright fluorescence. (a) TCSPC spectra of Cl-SiNPs, di-SiNPs, and ca-SiNPs (λ_{ex} = 365 nm; λ_{em} = emission maximum wavelength, 20 °C). (b) PL decay of di-SiNPs measured at different emission wavelengths. (c) Femtosecond time-resolved PL data of di-SiNPs and ca-SiNPs. (d) Scheme of the surface modification process leading to ultrabright PL.

and no fast decay can be observed in the femtosecond to picosecond PL decay kinetics. These results further demonstrate that the single highly emissive recombination channel results from such surface modification.

To obtain deeper insight into the highly emissive center induced by such surface modification in ca- and di-SiNPs, more kinds of SiNPs with different surfaces (1,2,3,4-tetrahydrocarbazole-, *N*-methylamine-, and propylamine-modified, and unmodified) were fabricated in the same manner, and their PL properties were investigated (as shown in Figures S10−S13). Compared with ca- and di-SiNPs, 1,2,3,4-tetrahydrocarbazole-modified SiNPs hold bright PL around 500 nm, with PLQYs down to 30% and a similar single-exponential decay with a 15 ns lifetime. For *N*-methylaniline-modified SiNPs, more significant decreases of PLQYs (10%) and a shorter FLT (10 ns) with a biexponential decay occur. The PL characteristics of propylamine-modified and unmodified SiNPs are much more different, which display deep blue PL with low PLQYs (<10%) and fast biexponential decays (FLT = 6 and 4 ns). Meanwhile, ca- and di-SiNPs display excitation-independent emissions (fixed emission peak under various excitations, details are shown in Figure S14), while emissions of other surface-modified SiNPs are more or less excitation-dependent. The excitation-independent PL of ca- and di-SiNPs suggests that the induced uniform emissive states dominate their PL process. However, for other surface-modified SiNPs whose capping agents have fewer or no N-linking phenyl rings, additional emissive channels may still contribute to the PL, or the induced emissive states are not uniform, which results in the excitation-dependent PL. Moreover, experiments show that the significant restriction of motion caused by the N-linking phenyl ring is also important to achieve high PLQYs, due to suppression of molecular-motion-based nonradiative relaxations. PL characteristics of all SiNPs with different surfaces are listed for comparison in Table S1. From the above results, it can be suggested that the N-linking phenyl ring in capping agents is essential for the formation of the highly emissive center of SiNPs. Furthermore, two phenyl rings linked by an N atom can make the induced emissive channel more competitive with other decay channels, leading to higher PLQYs, longer FLT with a single-exponential decay, and excitation-independent PL behavior.

On the other hand, control experiments in which Cl-SiNPs were reacted with diphenylamine or carbazole in the absence of air showed no such ultrabright PL, indicating that partial surface oxidation is crucial for ultrabright PL. Although the precise mechanism still needs further investigation (such as the detail role of oxidized sites, etc.), it can be suggested that the ultrabright cyan-green PL from our ca- and di-SiNPs is largely dependent on the structure of surface-attached organic agents and comes from the induced surface highly emissive center, which is probably based on the synergy between attached ligands and surface oxidized sites.

PL dynamic characteristics of di- and ca-SiNPs are another figure of merit that can be utilized. It is well-known that the typical monoexponential decay kinetics enable straightforward identification of dyes from measurements of FLTs, making dyes suitable for applications involving lifetime measurements. However, the lifetimes of common dyes are too short (usually less than 5 ns) for efficient temporal discrimination from scattering and cellular autofluorescence.[6a] On the other hand, typical QDs with relatively longer PL lifetimes always possess multiple-exponential decays, which severely hinders their applications involving lifetime measurements.[6b] Our surface-modified SiNPs, featuring both monoexponential decay behavior and a relatively longer PL lifetime, greatly satisfy the requirements for practical and accurate fluorescence lifetime imaging microscopy (FLIM).

The di-SiNPs, being sensitive to temperature, behave as extraordinary FLT nanothermometers. Variations of FLT in a wide temperature range from 0.5 to 60 °C were systematically investigated. As shown in Figure 4a, the FLT keeps decreasing from 23 ns down to 8 ns as the temperature increases from 0.5 to 60 °C. This temperature response range covers both the physiological temperature for biology studies and the working temperature for many electronic devices. The PL intensity also

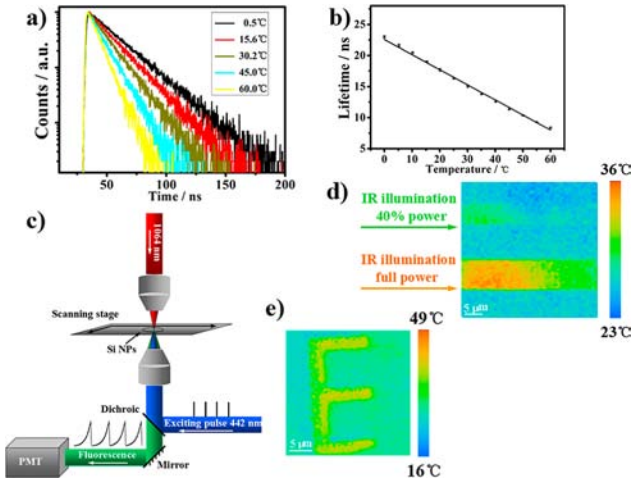

Figure 4. di-SiNPs act as excellent nanothermometers through the FLIM technique. (a) Fluorescence decay curves corresponding to di-SiNPs at different temperatures. (b) Temperature variation of FLT obtained for di-SiNPs. Dots are experimental data, and solid line is the best linear fit. (c) Schematic diagram of the experimental setup used to monitor local heating experiment. Scanning process was controlled by the scanning stage. (d) Pseudocolor thermal distribution images of the temperature-sensitive SiNPs aqueous solution. IR laser was used to change the temperature of different areas due to the fast local heating effect, which was controlled to turn on and off at different times during scanning. (e) Pseudocolor thermal imaging of a character pattern.

dx.doi.org/10.1021/ja407508v | *J. Am. Chem. Soc.* 2013, 135, 14924−14927

keeps decreasing as the temperature rises (Figure S15). Moreover, the FLT is found to decrease linearly with increasing temperature (Figure 4b). Thermal linearity is advantageous since it makes the correlation between lifetime and temperature straightforward and meanwhile provides a constant thermal sensitivity along the entire dynamic range.[5] The diphenylamine-modified SiNPs exhibit about 0.24 ns variations per degree centigrade, with a thermal resolution better than 1 °C. In addition, the di-SiNPs exhibit high stability and repeatability under elevated temperature (Figure S16). However, ca-SiNPs do not exhibit the same temperature-sensitive PL behavior as diphenylamine-modified ones (Figure S17). Generally, an increase in temperature results in a decrease in the PLQYs and FLT due to thermal agitation of nonradiative processes such as vibrations and rotations based on surface capping agents. Carbazole, holding a more rigid structure, significantly weakens such temperature effects.

Provided reasonable temperature-sensitive PL properties can be obtained, SiNPs have intrinsic advantages as nanothermometers that are desired in micro/nano electronics, integrated photonics, and biomedical applications due to their compatibility with conventional silicon technologies and excellent biocompatibility. The di-SiNPs, having high sensitivity, wide response range, robust stability and repeatability, monoexponential decay, linear temperature versus lifetime dependence, and relative long FLT, hold great potential as valuable nanothermometers. To demonstrate the ability of di-SiNPs to report thermal gradient images and measure the temperature variations localized to a micrometer-sized area, a time-domain FLT imaging setup with a 1064 nm IR heating beam was used (Figure 4c). Figure 4d shows the temperature distribution (23−36 °C) of aqueous solutions of SiNPs in 40 μm × 40 μm areas under local heating by the IR beam at 1064 nm. The image clearly shows the temperature distribution and the effect of local heating by the IR beam. Figure 4e presents a character pattern, the letter "E", made by evaporating Au on a SiO_2 substrate. Under the same heating conditions, temperature differences between the pattern and the surrounding matrix can be clearly reported by our SiNPs. The experimental results above demonstrate the ability of di-SiNPs to be used as nanothermometers through FLT imaging.

In conclusion, strongly enhanced fluorescence with PLQYs up to 75% can be obtained from SiNPs after a novel surface modification. The surface-modified SiNPs can be readily dispersed in aqueous solutions with high storage stability. Emergence of a single highly emissive recombination channel across the entire QD ensemble induced by surface modification is demonstrated. The single-exponential decay and relative long lifetime render the surface-modified SiNPs as promising candidates for FLT sensing and imaging. More importantly, experiments demonstrate that di-SiNPs can be utilized as excellent FLT nanothermometers, holding great promise for use in wide-ranging applications.

■ ASSOCIATED CONTENT

Supporting Information

Detailed synthesis protocols, experimental methods, Figures S1−S18, Table S1, and corresponding discussions. This material is available free of charge via the Internet at http://pubs.acs.org.

■ AUTHOR INFORMATION

Corresponding Author

zzshao@fudan.edu.cn

Notes

The authors declare no competing financial interest.

■ ACKNOWLEDGMENTS

This work is supported by the National Natural Science Foundation of China (No. 21034003), Program of Shanghai Subject Chief Scientist (12XD1401000), Shanghai Pujiang Program grant (11PJ1401000), and National Basic Research Program o China (2013CB934400 and 2012CB932400).

■ REFERENCES

(1) (a) Green, M. A.; Zhao, J.; Wang, A.; Reece, P. J.; Gal, M. *Nature* **2001**, *412*, 805. (b) Pavesi, L.; Dal Negro, L.; Mazzoleni, C.; Franzò, G.; Priolo, F. *Nature* **2000**, *408*, 440. (c) Cheng, K. Y.; Anthony, R.; Kortshagen, U. R.; Holmes, R. J. *Nano Lett.* **2010**, *10*, 1154. (d) Ding, Z.; Quinn, B. M.; Haram, S. K.; Pell, L. E.; Korgel, B. A.; Bard, A. J. *Science* **2002**, *296*, 1293. (e) Guan, M.; Wang, W. D.; Henderson, E. J.; Dag, O.; Kubel, C.; Chakravadhanula, V. S. K.; Rinck, J.; Moudrakovski, I. L.; Thomson, J.; McDowell, J.; Powell, A. K.; Zhang, H. X.; Ozin, G. A. *J. Am. Chem. Soc.* **2012**, *134*, 8439. (f) Shiohara, A.; Hanada, S.; Prabakar, S.; Fujioka, K.; Lim, T. H.; Yamamoto, K.; Northcote, P.; Tilley, R. D. *J. Am. Chem. Soc.* **2010**, *132*, 248. (g) Atkins, T. M.; Thibert, A.; Larsen, D. S.; Dey, S.; Browning, N. D.; Kauzlarich, S. M. *J. Am. Chem. Soc.* **2011**, *133*, 20664.

(2) (a) Puzzo, D. P.; Henderson, E. J.; Helander, M. G.; Wang, Z.; Ozin, G. A.; Lu, Z. *Nano Lett.* **2011**, *11*, 1585. (b) He, Y.; Su, Y. Y.; Yang, X. B.; Kang, Z. H.; Xu, T. T. R.; Zhang, Q.; Fan, C. H.; Lee, S. T. *J. Am. Chem. Soc.* **2009**, *131*, 4434. (c) *Silicon Nanocrystals: Fundamentals, Synthesis and Applications*; Pavesi, L., Turan, R., Eds.; Wiley-VCH: Weinheim, 2010. (d) Erogbogbo, F.; Yong, K. T.; Roy, I.; Hu, R.; Law, W. C.; Zhao, W. W.; Ding, H.; Wu, F.; Kumar, R.; Swihart, M.; Prasad, P. N. *ACS Nano* **2011**, *5*, 413. (e) Sato, K.; Yokosuka, S.; Takigami, Y.; Hirakuri, K.; Fujioka, K.; Manome, Y.; Sukegawa, H.; Iwai, H.; Fukata, N. *J. Am. Chem. Soc.* **2011**, *133*, 18626. (f) He, Y.; Zhong, Y. Y.; Peng, F.; Wei, X. P.; Su, Y. Y.; Lu, Y. M.; Su, S.; Gu, W.; Liao, L. S.; Lee, S. T. *J. Am. Chem. Soc.* **2011**, *133*, 14192.

(3) (a) Erogbogbo, F.; Chang, C. W.; May, J.; Prasadbc, P. N.; Swihart, M. T. *Nanoscale* **2012**, *4*, 5163. (b) Kusová, K.; Cibulka, O.; Dohnalova, K.; Pelant, I.; Valenta, J.; Fucikova, A.; Zidek, K.; Lang, J.; Englich, J.; Matejka, P.; Stepanek, P.; Bakardjieva, S. *ACS Nano* **2010**, *4*, 4495.

(4) (a) Ye, F.; Wu, C.; Jin, Y.; Chan, Y.-H.; Zhang, X.; Chiu, D. T. *J. Am. Chem. Soc.* **2011**, *133*, 8146. (b) Yang, J.-M.; Yang, H.; Lin, L. *ACS Nano* **2011**, *5*, 5067. (c) Maestro, L. M.; Rodríguez, E. M.; Iglesias-de la Cruz, F. S. M. C.; Juarranz, A.; Naccache, R.; Vetrone, F.; Jaque, D.; Capobianco, J. A.; Sole, J. G. *Nano Lett.* **2010**, *10*, 5109.

(5) (a) Jaque, D.; Vetrone, F. *Nanoscale* **2012**, *4*, 4301. (b) Brites, C. D. S.; Lima, P. P. N.; Silva, J. O.; Millan, A.; Amaral, V. S.; Palacio, F.; Carlos, L. D. *Nanoscale* **2012**, *4*, 4799.

(6) (a) Berezin, M. Y.; Achilefu, S. *Chem. Rev.* **2010**, *110*, 2641. (b) Resch-Genger, U.; Grabolle, M.; Cavaliere-Jaricot, S.; Nitschke, R.; Nann, T. *Nature Methods* **2008**, *5*, 763.

(7) (a) Baldwin, R. K.; Pettigrew, K. A.; Ratai, E.; Augustine, M. P.; Kauzlarich, S. M. *Chem. Commun.* **2002**, 1822. (b) Zou, J.; Baldwin, R. K.; Pettigrew, K. A.; Kauzlarich, S. M. *Nano Lett.* **2004**, *4*, 1181.

(8) Dasog, M.; Yang, Z.; Regli, S.; Atkins, T. M.; Faramus, A.; Singh, M. P.; Muthuswamy, E.; Kauzlarich, S. M.; Tilley, R. D.; Veinot, J. G. C. *ACS Nano* **2013**, *7*, 2676.

(9) (a) Kang, Z. H.; Liu, Y.; Tsang, C. H. A.; Ma, D. D. D.; Fan, X.; Wong, N.-B.; Lee, S. T. *Adv. Mater.* **2009**, *21*, 661. (b) Kumar, V. *Nanosilicon*; Elsevier Ltd.: Amsterdam, 2007.

(10) (a) Anthony, R. J.; Rowe, D. J.; Stein, M.; Yang, J.; Kortshagen, U. *Adv. Funct. Mater.* **2011**, *21*, 4042. (b) Jurbergs, D.; Rogojina, E.; Mangolini, L.; Kortshagen, U. *Appl. Phys. Lett.* **2006**, *88*, 233116.

(11) Atkins, T. M.; Cassidy, M. C.; Lee, M.; Ganguly, S.; Marcus, C. M.; Kauzlarich, S. M. *ACS Nano* **2013**, *7*, 1609.